# Effects of Side Wall Inclination Angle on Transition Mixed Convection in a Lid-Driven Trapezoidal Cavity

**Enamul Hasan Rozin, Hasib Ahmed Prince, Emdadul Haque Chowdhury and Sumon Saha**
Department of Mechanical Engineering
Bangladesh University of Engineering and Technology
Dhaka-1000, Bangladesh
enamulrozin4@gmail.com, prince.hap77@gmail.com, shoikot1151153@gmail.com,
sumonsaha@me.buet.ac.bd

## Abstract

The influence of various side wall inclination angles on the flow transition from laminar to chaos region in pure mixed convection heat transfer in a lid-driven trapezoidal cavity has been numerically investigated in this study. The governing non-dimensional Navier-Stokes and thermal energy equations are solved using the Galerkin weighted residual finite element method. The study explores the effects of different inclination angles of the two side walls from $0^{\circ}$ to $30^{\circ}$ over the transition characteristics, maintaining a constant cross-sectional area of the cavity. The overall investigation is carried out in the pure mixed convection regime, simultaneously varying the Reynolds and the Grashof numbers within the range of $10^{-1}$ to $10^{3}$ and $10^{-2}$ to $10^{6,}$ respectively. The isotherm contours and streamline plots at local maximum, and minimum points of the chaos regions are introduced. The heat transfer performance inside the cavity is quantified by obtaining the average Nusselt number along the bottom heated surface. It is found that the transition occurs at a higher *Re* with the increase of the sidewall inclination angle. Two chaos regions are observed in the case of larger inclination angles. However, for small inclination angles, only one chaos region is found.

## Keywords
Transition mixed convection, Laminar flow, Finite element method, Nusselt number and Trapezoidal cavity.

## 1. Introduction

Mixed convective flow in a lid-driven cavity exists in many industrial applications, where both forced convection and natural convection play a major role. Recently, it becomes one of the most common topics among researchers and engineers with its widespread usages in many engineering and industrial fields, including heat exchangers, lubrication technologies, drying technology, food processing industries, float glass output and heat transfer in solar pans, solar collectors, nuclear heat hydraulics, cooling of electronics and so on. Numerical and experimental research on mixed convective flow in lid-driven cavities has been performed in the past. In various applications such as attic spaces in homes, greenhouses or crop drying, etc., non-rectangular shapes such as trapezoidal, arc-shaped, prismatic cavities filled with fluid particles have a substantial impact on flow and temperature profiles in mixed convection.

### 1.1 Literature Review

There are several numbers of authors who paid attention to mixed convection on the trapezoidal cavity. Alleborn *et al.* (1999) investigated the lid-driven cavity where both the cold bottom wall and the hot top wall were in a constant velocity, and the double-diffusive phenomena were observed. Mamun et al. (2010) also studied the mixed convection characteristics of an inclined lid-driven trapezoidal cavity using the finite volume method (FVM). Abu-Nada (2010) numerically examined the mixed convection in an inclined square cavity by observing the effects of nanofluid. Cheng (2011) analyzed the mixed convection in a lid-driven square cavity, and the effect of Reynolds numbers, Grashod number, Prandtl number were reported. Saha *et al.* (2014) studied the characteristics of changes from laminar to chaos area in pure mixed convection of a lid-driven trapezoidal cavity filled with $Al_2O_3$-water nanofluid. Esfe *et al.* (2014) estimated the impact of $Al_2O_3$-water nanofluid's properties on mixed convection heat transfer and fluid flow in an inclined double lid-driven square enclosure with sinusoidal temperature distribution on the left wall and constant temperature on the right wall of the cavity. Hasib *et al.* (2015) showed the influence of tilt angle on flow and thermal fields, heat transfer characteristics, etc., for pure mixed convection regime ($Ri$ = 1) in two different trapezoidal configurations filled with $Al_2O_3$-water nanofluid. Azam *et al.* (2016) studied the transition phenomena from laminar to chaos in an MHD mixed convection case at Richardson number of a lid-driven trapezoidal enclosure filled with

*Cu*-water nanofluid. Taamneh and Bataineh (2017) investigated the effect of Richardson number, the volume fraction of nanoparticles on heat transfer, and fluid flow in a square cavity. The cavity was filled with $Al_2O_3$-water nanofluid, and the hot top wall was lid-driven. Subedi *et al.* (2017) studied the impact of the interior angle at *Ri* = 1 on the transition from laminar to chaos area in a lid-driven parallelogram cavity filled with water. Therefore, investigation on mixed convection in any lid-driven cavity has got the attention of many researchers for its importance in different practical aspects.

### 1.2 Objectives

It is observed that several studies were conducted on mixed convection heat transfer in different cavities with moving lids. However, as per the authors' knowledge, no studies are done yet observing the effects of the inclination angle of a lid-driven trapezoidal cavity laminar on the laminar to chaos created in transition mixed convection phenomena. Therefore, the aim of the present work is to investigate the effect of the sidewall inclination angle of a trapezoidal cavity on the transition region (laminar to chaos) filled with water as working fluid by evaluating the magnitude of average Nusselt number.

## 2. Computational Model Description

The physical domain considered in the present model along with the boundary conditions is demonstrated in figure 1. The length of the bottom horizontal wall of the cavity is *L*, and $\gamma$ is the angle of inclination of the side walls with the y-axis. The top and the bottom surfaces of the enclosure are subjected to a constant lower ($T_c$) and higher temperature ($T_h$), respectively, while the side inclined walls are considered to be insulated. All the cavity boundaries are stationary except for the top surface, which is allowed to move along the positive x-direction at a constant speed of $u_0$. Seven different inclination angles ($\gamma = 0°, 5°, 10°, 15°, 20°, 25°,$ and $30°$) are considered for the current investigation. The area of the cavity is denoted by $A_c$, and the non-dimensional area ($A_c\ /H^2$) is kept fixed at ($A_c\ /H^2$) = 1.0 for the whole investigation.

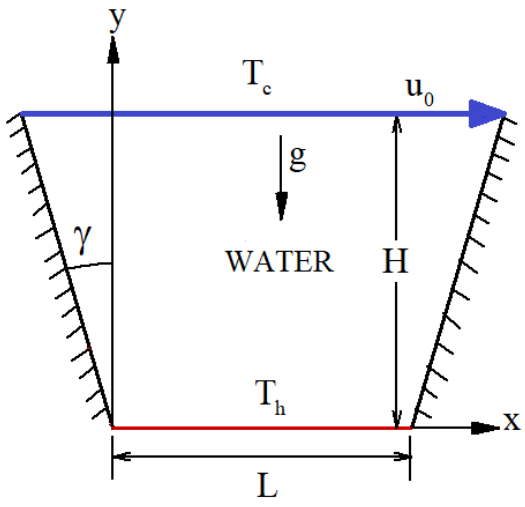


**Figure 1.** Schematic diagram of the lid-driven trapezoidal cavity

Water is taken as the working fluid and considered as an incompressible Newtonian fluid. The density variation of water with temperature is addressed by obeying the Boussinesq approximation in the momentum equation, while all other thermo-physical properties are considered to be constant. Viscous dissipation, radiation effect, and internal heat generation are neglected in the energy equation. In the light of these assumptions, the non-dimensional forms of two-dimensional steady-state continuity, momentum, and energy equations can be expressed in the Cartesian coordinate system as,

$$\frac{\partial U}{\partial X} + \frac{\partial V}{\partial Y} = 0, \tag{1}$$

$$U\frac{\partial U}{\partial X}+V\frac{\partial U}{\partial Y}=-\frac{\partial P}{\partial X}+\frac{1}{Re}\left(\frac{\partial^2 U}{\partial X^2}+\frac{\partial^2 U}{\partial Y^2}\right), \tag{2}$$

$$U\frac{\partial V}{\partial X}+V\frac{\partial V}{\partial Y}=-\frac{\partial P}{\partial Y}+\frac{1}{Re}\left(\frac{\partial^2 V}{\partial X^2}+\frac{\partial^2 V}{\partial Y^2}\right)+Ri\Theta, \tag{3}$$

$$U\frac{\partial \Theta}{\partial X}+V\frac{\partial \Theta}{\partial Y}=\frac{1}{RePr}\left(\frac{\partial^2 \Theta}{\partial X^2}+\frac{\partial^2 \Theta}{\partial Y^2}\right). \tag{4}$$

Equations (1-4) are dimensionless. The scales used to obtain these equations are defined as,

$$X=\frac{x}{H}, Y=\frac{y}{H}, U=\frac{u}{u_0}, V=\frac{v}{u_o}, P=\frac{p}{\rho u_0^{\,2}}, \Theta=\frac{T-T_c}{T_h-T_c}.. \tag{5}$$

Here, $x$ and $y$ are the coordinates in the Cartesian system, $u$ and $v$ are the velocity components, $P$ is the pressure, $T$ is the temperature, $X$ and $Y$ are the non-dimensional coordinates, $U$ and $V$ are the dimensionless velocity components in $X$- and $Y$-directions, $\Theta$ is the dimensionless temperature, $P$ is the dimensionless pressure. The governing parameters used in equations (2-4) are Reynolds number ($Re$), Grashof number ($Gr$), Prandtl number ($Pr$), and Richardson number ($Ri$), and which are expressed as:

$$Re=\frac{u_o H}{\nu}, Gr=\frac{g\beta\left(T_h-T_c\right)H^3}{\nu^2}, Pr=\frac{\nu}{\alpha}, Ri=\frac{Gr}{Re^2}.. \tag{6}$$

Here, $\alpha$ is the thermal diffusivity of the water, $\nu$ is the kinematic viscosity of water, $g$ is the gravitational acceleration and $\beta$ is the coefficient of thermal expansion for water. The properties of water are given in table 1.

**Table 1.** Thermo-physical properties of water at 20°C

| **Properties** | **Water** |
|---|---|
| $C_p$ [J/(kg.K)] | 4179 |
| $\rho$ [kg/m$^3$] | 997.1 |
| $k$ [W/m.K] | 0.613 |
| $\beta$ [1/K] | $2.1\times10^{-4}$ |
| $\mu$ [kg/m] | $1.002\times10^{-3}$ |
| $Pr$ [-] | 6.83 |

The non-dimensional boundary conditions used for the present investigation are shown in table 2.

**Table 2.** Non-dimensional boundary conditions

| **Boundary wall** | **Thermal field** | **Velocity field** |
|---|---|---|
| Top wall | $\Theta=0$ (cold) | $U=1, V=0$ |
| Bottom wall | $\Theta=1$ (hot) | $U=V=0$ |
| Left and right walls | $\frac{\partial\Theta}{\partial n}=0$ (insulated) | $U=V=0$ |

The average Nusselt number calculated along the bottom heated surface can be expressed as,

$$Nu = -\frac{H}{L}\int_0^{L/H}\frac{\partial\Theta}{\partial Y}dX. \quad (7)$$

## 3. Simulation Procedure

The non-dimensional governing equations are solved using the finite element method. The whole domain is discretized using both non-uniform triangular and quadrilateral elements, and a relatively finer mesh is applied near the boundaries. The relative tolerance for the error criteria is used to be $10^{-6}$.

A mesh sensitivity test is carried out to get the results with reasonable accuracy and less computational time. In the current study, it is done for $\gamma = 10°$, $Re = 50$, and $Ri = 1$, which is illustrated in table 3. It is seen that with increasing the number of elements, the average Nusselt number, $Nu$ converges to a constant value, and 6911 is found as the optimum number of elements.

For any numerical simulation, the model is validated against the previous published results. Present model is validated with the work of Saha *et al.* (2014), where the simulation was done in a trapezoidal cavity of aspect ratio equal to 0.732 and filled with water-$Al_2O_3$ nanofluid. Validation was performed at $Ri = 1$ and $\phi = 0$, as is illustrated in figure 2.

**Table 3.** Mesh independent test for $\gamma = 10°$, $Re = 50$, $Ri = 1$.

| No. of elements | *Nu* |
|---|---|
| 1500 | 4.7259 |
| 2507 | 4.7401 |
| 4601 | 4.7539 |
| **6911 (optimum)** | **4.7652** |
| 7849 | 4.7657 |

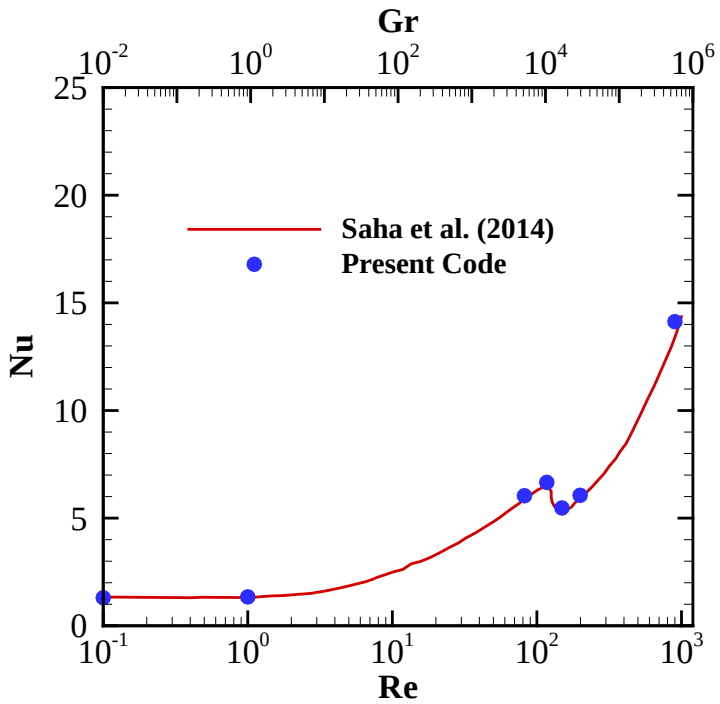


**Figure 2.** Comparison of average Nusselt number versus Reynolds number between the present model and Saha *et al.* (2014) at $Ri = 1$ and solid volume fraction, $\phi = 0$

## 4. Results and Discussion

The present study explores the influence of sidewall inclination angle over pure mixed convection within a lid-driven trapezoidal chamber for water. The reason behind the choice of the trapezoidal enclosure is that Chowdhury et al. (2009) suggested the trapezoidal cavity to be more effective in terms of heat transfer performance than the square cavity. Numerical simulations have been performed considering seven different inclination angles which are $\gamma = 0^o$, 5°, 10°, 15°, 20°, 25°, and 30°. The Richardson number is kept constant at unity to ensure pure mixed convection. The Reynolds number is varied within $10^{-1} \leq Re \leq 10^3$ while the Grashof number is varied accordingly in the range of $10^{-2} \leq Gr \leq 10^6$ to keep Richardson number, $Ri = 1$. Based on the observation of the average Nusselt number versus Reynold number plots, which indicates the change of flow from laminar to chaos, the above ranges of Reynolds number and Grashof numbers are chosen.

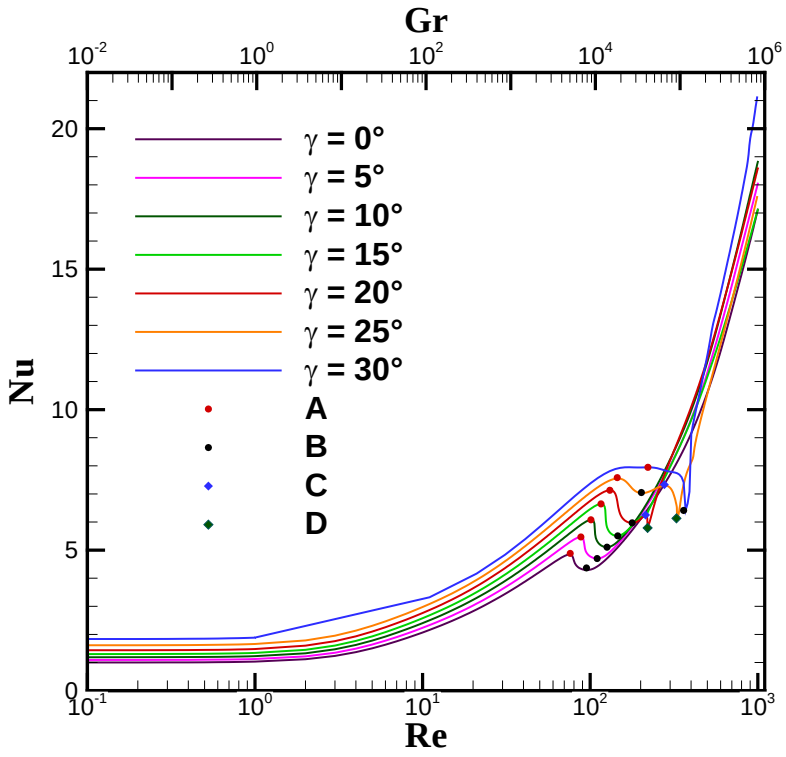


**Figure 3.** Variations of average Nusselt number with Reynolds number and Grashof number for different inclination angles of the trapezoidal cavity.

Figure 3 portrays the combined effects of the variation of *Re* and *Gr* on the average Nusselt number for different $\gamma$. After Re = 10, the stiffness of the curve starts to alter since the dominant mode of heat transfer shifts from conduction to convection, which is within the laminar zone. For all the inclination angles, a sudden but gradual drop of *Nu* is observed, which indicates the flow transition from laminar to chaos region. Afterward, Nu continues to increase with increasing *Re*. Note that for inclination angles, $\gamma = 0°$ to 30°, *Nu* suddenly decreases from the local maximum (*A*) to the local minimum (*B*) points i.e., there is only one chaos region is observed for these angles. On the other hand, for inclination angles, $\gamma = 20°$ and 25°, after the first chaos, another instantaneous drop in *Nu* is found from the local maximum (*C*) to the local minimum (*D*), indicating a second chaos region for these two angles. It is worth mentioning that with the increase in inclination angle, the chaos region shifts rightward. That is why the transition begins at a higher value of *Re* for the increased inclination angle of the cavity.

Figure 3 reveals that for lower inclination angle such as $\gamma = 0°$ to 15°, there is only one chaos region. The further increment in inclination angle causes multiple chaotic region. For $\gamma = 20°$ and 25°, there are two chaos regions. The summary of all critical parameters (Reynolds number and average Nusselt number) at the local maximum (*A*) and minimum (*B*) points for $\gamma = 0^o$, 5°, 10°, 15° and 30° that lead to flow regime laminar to chaos is presented in table 4.

The summary of critical parameters at the local maximum (*A*) and minimum (*B*) points of first chaos and local maximum (*C*) and minimum (*D*) points of second chaos for $\gamma = 20^{o}$ and 25° that lead to flow regime laminar to chaos is presented in table 5.

**Table 4.** List of critical parameters for the transition from laminar to only chaos for $\gamma$ = 0°, 5°, 10°, 15°, 30°

| Inclination angle | $Re\ (A)$ | $Re\ (B)$ | $Nu\ (A)$ | $Nu\ (B)$ | $\Delta Nu\ (A-B)$ |
|---|---|---|---|---|---|
| 0° | 76 | 95 | 4.8828 | 4.3659 | 0.5169 |
| 5° | 88 | 110 | 5.4675 | 4.7002 | 0.7673 |
| 10° | 101 | 126 | 6.0791 | 5.1043 | 0.9748 |
| 15° | 116 | 146 | 6.6447 | 5.5072 | 1.1375 |
| 30° | 221 | 361 | 7.9471 | 6.4117 | 1.5354 |

**Table 5.** List of critical parameters for the transition from laminar to both chaos regions for $\gamma$ = 20° and 25°

| Inclination angle | $Re\ (A)$ | $Re\ (B)$ | $Nu\ (A)$ | $Nu\ (B)$ | $\Delta Nu\ (A-B)$ | $Re\ (C)$ | $Re\ (D)$ | $Nu\ (C)$ | $Nu\ (D)$ | $\Delta Nu\ (C-D)$ |
|---|---|---|---|---|---|---|---|---|---|---|
| 20° | 131 | 178 | 7.13 | 5.97 | 1.16 | 214 | 220 | 6.25 | 5.79 | 0.46 |
| 25° | 145 | 202 | 7.58 | 7.05 | 0.53 | 277 | 327 | 7.33 | 6.13 | 1.2 |

One can observe from table 4 and 5 that up to $\gamma = 20^{0}$, not only the transition begins at a higher value of *Re*, but also the difference in *Nu* increases with increasing inclination angle. After $\gamma = 20°$, the drop of average Nusselt number at the first chaos region becomes smaller, and the drop of the average Nusselt number at the second chaos region becomes larger with the increase of inclination angle, which is clearly found for $\gamma = 25°$. For $\gamma = 30°$, the chaos region for the lower Reynolds number vanishes, and there remains only one chaos region.

The variations of streamlines and isothermal contours at local maximum and minimum points of chaos regions for inclination angles, $\gamma = 15°$, 30°, and 25° are depicted in figures 4 and 5, respectively, to profoundly understand the changes in flow and thermal fields within the chaos regions.

From the streamline plots in figure 4, it is apparent that irrespective of inclination angles, a clockwise single-core circulating vortex is generated inside the cavity due to the rightward moving lid, which is presented by the negative values of stream functions. As $\gamma$ increases, the strength of the circulation increases a bit. Also, note that, at point A, the circulating vortex occupies a larger area inside the cavity. At B point, however, the circulation zone gets congested near the cold wall due to the increase of thermal boundary layer thickness near the hot wall, indicating a decrease in heat transfer.

The clockwise circulating vortex pushes the isotherms at the bottom and left boundaries of the cavity (Figure 4). No noticeable difference in the thermal field distribution is observed with increasing inclination angle. However, as mentioned earlier, the thickness of the thermal boundary layer at point B is much higher than that of point A, which results in lowering the value of *Nu* at point B.

Comparing the streamline patterns for $\gamma = 15°$ and $30^{0}$, it can be inferred that the circulation strength is much higher at $\gamma = 30^{0}$ than that of $\gamma = 15^{0}$, which is also evident from the smaller thermal boundary layer thickness of $\gamma = 30^{0}$ from the isotherms plot. As mentioned earlier, the vortex occupies more area at point A relative to point B, indicating a larger hydrodynamic boundary layer thickness at point B, and thus, a decreased heat transfer performance. A similar

conclusion can also be derived by comparing the isotherms at point A and point B, as the thickness of the thermal boundary layer is larger at point B.

Figures 6 and 7 depicts the isotherms and streamlines at $\gamma = 20^0$ and $\gamma = 25^0$, respectively. As can be seen, the thickness of both the hydrodynamic and thermal boundary layers are substantially smaller for $\gamma = 25^0$ than that of $\gamma = 20^0$, indicating an enhanced heat transfer performance.

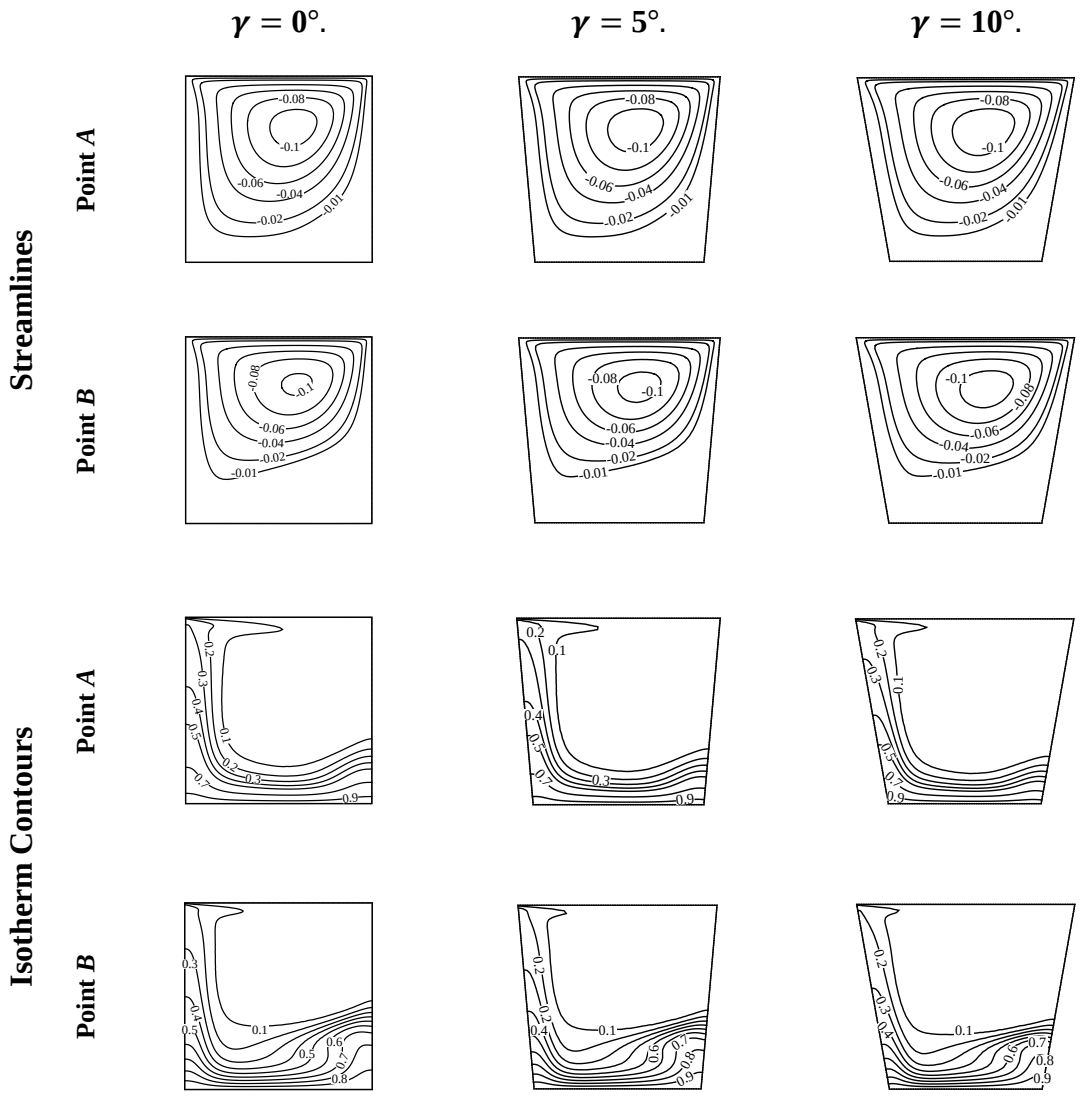


**Figure 4.** Streamlines and isotherm contours at local maximum and minimum points of chaos region for $\gamma = 0°, 5°, 10°$

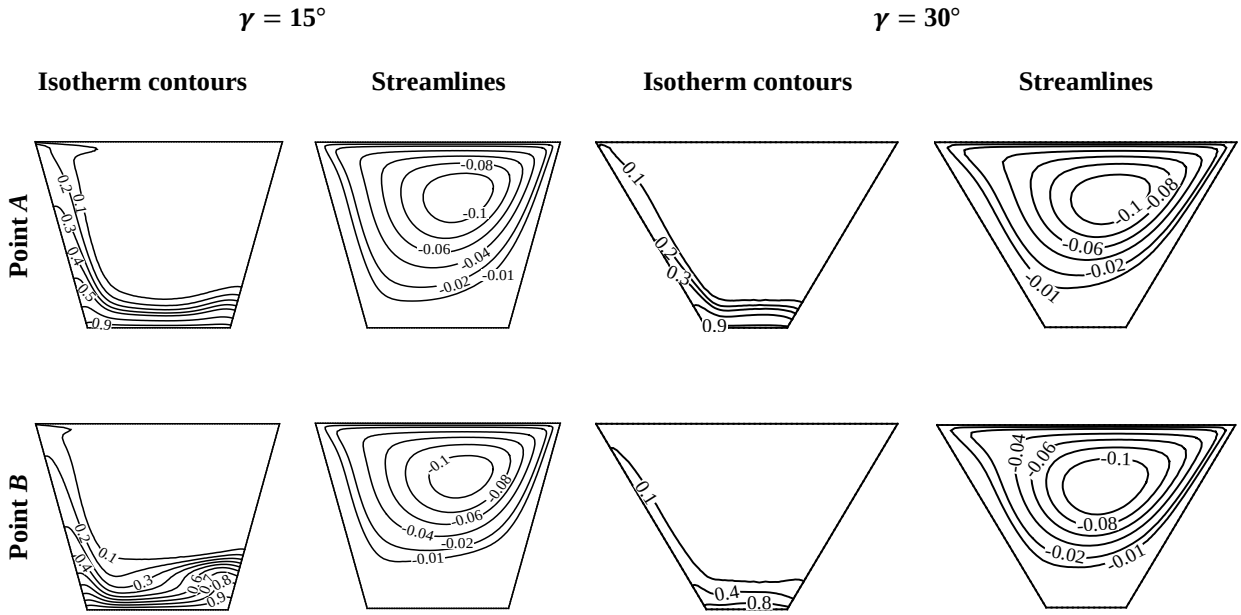


**Figure 5.** Streamlines and isotherm contours at local maximum and minimum points of chaos region for $\gamma = 15°$, 30°

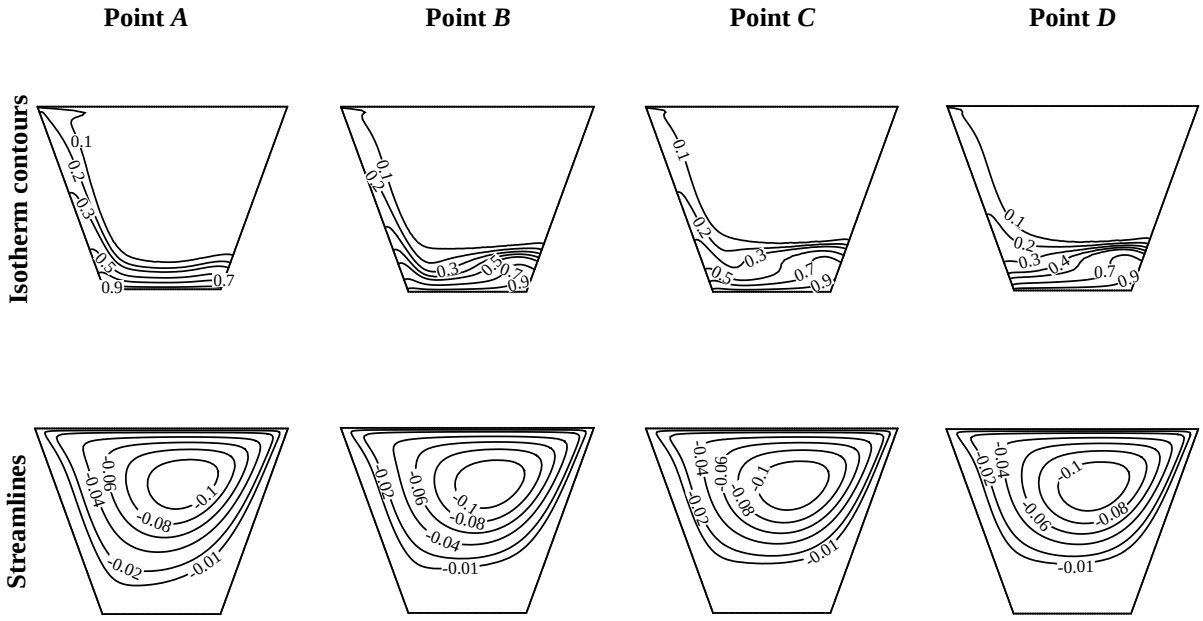


**Figure 6.** Streamlines and isotherm contours at local maximum and minimum points of chaos regions for $\gamma = 20°$

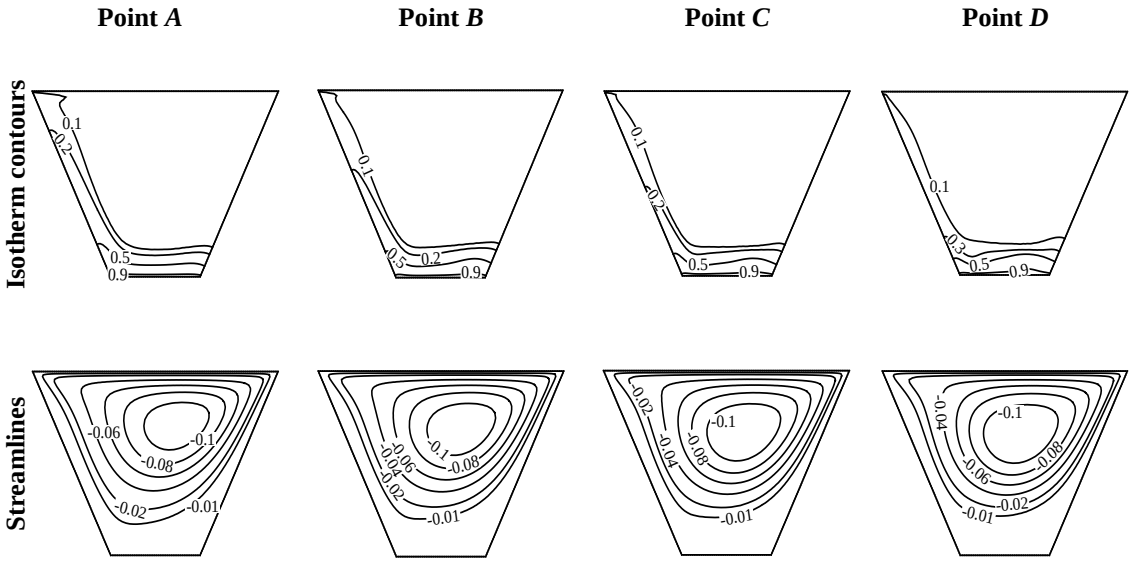


**Figure 7.** Streamlines and isotherm contours at local maximum and minimum points of chaos regions for $\gamma = 25°$.

## 5. Conclusion

The present study offers a comprehensive analysis of pure mixed convection in a trapezoidal cavity filled with water to observe the effect of different inclination angles of the side walls over the chaos region. The Richardson number is kept constant at unity, while varying the Reynolds and Grashof numbers in the range of $10^{-1} \leq Re \leq 10^3$ and $10^{-2} \leq Gr \leq 10^6$, respectively. Seven different inclination angles that are $\gamma = 0°, 5°, 10°, 15°, 20°, 25°,$ and $30°$ are considered to observe the effect of inclination angle over the flow and heat transfer characteristics in the present model. After *Re* = 10, the average Nusselt number starts to increase rapidly with increasing *Re*, as the mode of heat transfer shifts from conduction to convection. A sudden drop in *Nu* is observed at the local maximum point of the chaos region. The strength of this sharp drop depends on the inclination angle of the trapezoidal cavity. There is only one chaos region is found for inclination angles smaller than 20°. After that, a second chaos region appears, and it gets stronger with the further increase of inclination angle while the first one continuously gets weaker. The first chaos gets totally vanished when the inclination angle reaches 30°. With increasing inclination angle, the heat transfer performance increases, and the transition region experience a right shift. As the inclination angle increases, the strength of the circulation inside the cavity increases, and the thickness of both hydrodynamic and thermal boundary layers decreases. In short, this study discloses some important characteristics of the thermal and flow pattern inside a trapezoidal cavity with varying interior angles of the sidewalls, which will aid the researchers and engineers to design such enclosures in a more efficient way.

## Acknowledgements

The authors would like to express gratitude to the Department of Mechanical Engineering, Bangladesh University of Engineering and Technology (BUET), for providing continuous encouragement and necessary facilities throughout the research work. The authors would also like to thank their friend and colleague, Md. Habibur Rahman for his help during this investigation.

## References

Alleborn, N., Raszillier, H. and Durst, F., Lid driven cavity with heat and mass transport, *International Journal of Heat and Mass Transfer*, vol. 42(5), pp. 833–853, 1999.

Esfe, M. H., Akbari, M., Toghraie, D. S., Karimipour, A. and Afrand, M., Effect of nanofluid variable properties on

mixed convection flow and heat transfer in an inclined two-sided lid driven cavity with sinusoidal heating on sidewalls, *Heat Transfer Research*, vol. 45(5), pp. 409–432, 2014.

Hasib, M. H., Hossen, M. S. and Saha, S., Effect of tilt angle on pure mixed convection flow in trapezoidal cavities filled with water-$Al_2O_3$ nanofluid, *Procedia Engineering*, vol. 105, pp. 388–397, 2015.

Taamneh, Y. and Bataineh, K., Mixed convection heat transfer in a square lid driven cavity filled with $Al_2O_3$-water nanofluid, *Strojniški vestnik - Journal of Mechanical Engineering*, vol. 63(6), pp. 383–393, 2017.

Subedi, S., Barua, S., Hasan, M. A., Saha, S. and Islam, M. Q., Influence of interior angle on pure mixed convection of lid-driven parallelogram cavity, *AIP Conference Proceedings*, vol. 1851, pp. 020106, 2017.

Saha, S., Hossen, S., Hasib, M. H. and Saha, S. C., Onset of transition in mixed convection of a lid driven trapezoidal enclosure filled with water-$Al_2O_3$ nanofluid, *proceedings of 19th Australasian Fluid Mechanics Conference*, Melbourne, Australia, December 8-11, 2014.

Azam, M., Hasanuzzaman, M. and Saha, S., Onset of transition from laminar to chaos in mixed convection of a lid driven trapezoidal enclosure filled with Cu-water nanofluid, *AIP Conference Proceedings*, vol. 1754, pp. 050049, 2016.

Chowdhury, M. N. H. K., Saha, S. and Mamun, M. A. H., Mixed convection analysis in a lid driven trapezoidal cavity with isothermal heating at bottom for various aspect angles, *Proceedings of 8th International Conference on Mechanical Engineering*, Dhaka, Bangladesh, December 26-28, 2009.

Mamun, M. A. H., Tanim, T. R., Rahman, M. M., Saidur, R. and Nagata, S., Mixed convection analysis in trapezoidal cavity with a moving lid, *Int. J. Mech. Mater. Eng.*, vol. 5, pp. 18-28, 2010.

Cheng, T., Characteristics of mixed convection heat transfer in a lid-driven square cavity with various richardson and prandtl numbers, *Int. J. Therm. Sci.*, vol. 50, pp. 197-205, 2011.

Abu-Nada, E. and Chamkha, A. J., Mixed convection flow in a lid-driven inclined square enclosure filled with a nanofluid, *Euro. J. Mech. B/Fluids*, vol. 29, pp. 472-482, 2010.

## Biographies

**Enamul Hasan Rozin** is a citizen of Bangladesh who is currently living in Dhaka, Bangladesh. He is pursuing his B. Sc. Engg. Degree in Mechanical Engineering at the Bangladesh University of Engineering and Technology. His research interests include heat and mass transfer, computational fluid mechanics, molecular dynamics, artificial neural network (ANN). He has some publications in different international conferences.

**Hasib Ahmed Prince** is currently pursuing his B. Sc. Engg. Degree in mechanical engineering from the Department of Mechanical Engineering at Bangladesh University of Engineering and Technology. He has completed his secondary school certificate examination from Bangladesh Navy School, Chattogram, and higher secondary school certificate examination from Chattogram College under the board of intermediate and secondary education, Bangladesh. His research interests include computational heat and mass transfer, thermo-fluid mechanics, biomedical engineering, robotics and manufacturing operations, and artificial neural network. He has published and presented several research papers, posters, and projects in these fields already in different international conferences and competitions organized by different leading international organizations of engineers.

**Emdadul Haque Chowdhury** is an undergraduate student in the Department of Mechanical Engineering at Bangladesh University of Engineering and Technology (BUET), Dhaka, Bangladesh. He has published some journal and conference papers in different recognized journals and international conferences. Mr. Chowdhury has completed research projects on turbulent flow, computational fluid dynamics (CFD), computational heat transfer (CHT), and nanomaterials.

**Sumon Saha** is an Associate Professor in the Department of Mechanical Engineering at Bangladesh University of Engineering and Technology (BUET), Dhaka, Bangladesh. He earned B.Sc. Engg. in Mechanical Engineering from BUET, M. Sc. Engg. in Mechanical Engineering from BUET, and Ph.D. in Mechanical Engineering from the University of Melbourne, VIC, Australia. Dr. Saha has been working as a reviewer in several international journals including, Mathematical and Computer Modelling; Computers and Mathematics with Application; International Journal of Heat and Fluid Flow (Elsevier), International Journal of Engineering (IJE), Indian Journal of Mathematics (IJM), etc. He is a Life Member of Bangladesh Solar Energy Society, Membership No. L 86 and an Ex-Member of Institute of Engineers, Bangladesh, Membership No. M 21736; Ex-Member of Bangladesh Society of Mechanical Engineers, Membership No. M 05 004 ME. Dr. Saha has received many professional awards like International Postgraduate Research Scholarship (IPRS) [March 2009- December 2013] by the Australian federal government; Melbourne International Research Scholarship (MIRS) [March 2009- June 2013] by the University of Melbourne; RHD Studentship [June 2013] by University of Melbourne, and so on. His research interests include turbulent flow, computational fluid dynamics (CFD), and computational heat transfer (CHT).